

Recombination onto Doubly-Ionized Carbon in M17

(Old dog; new trick)

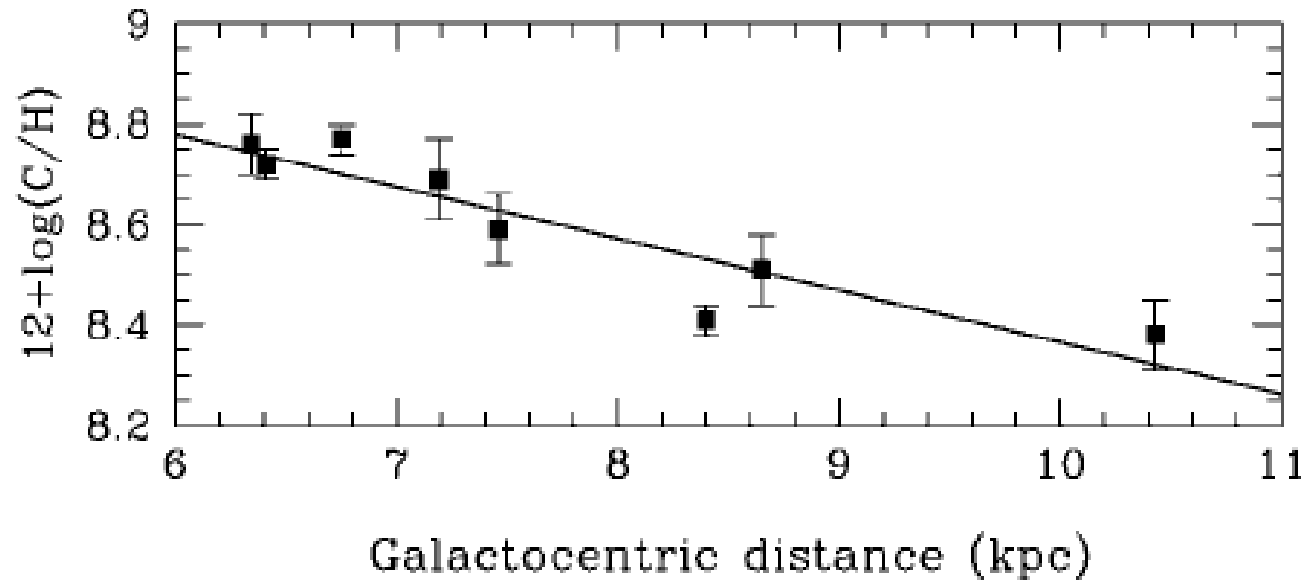
L. J Rickard, B. McEwen, and Y. Pihlström
(University of New Mexico)

New Mexico Symposium
4 November, 2016



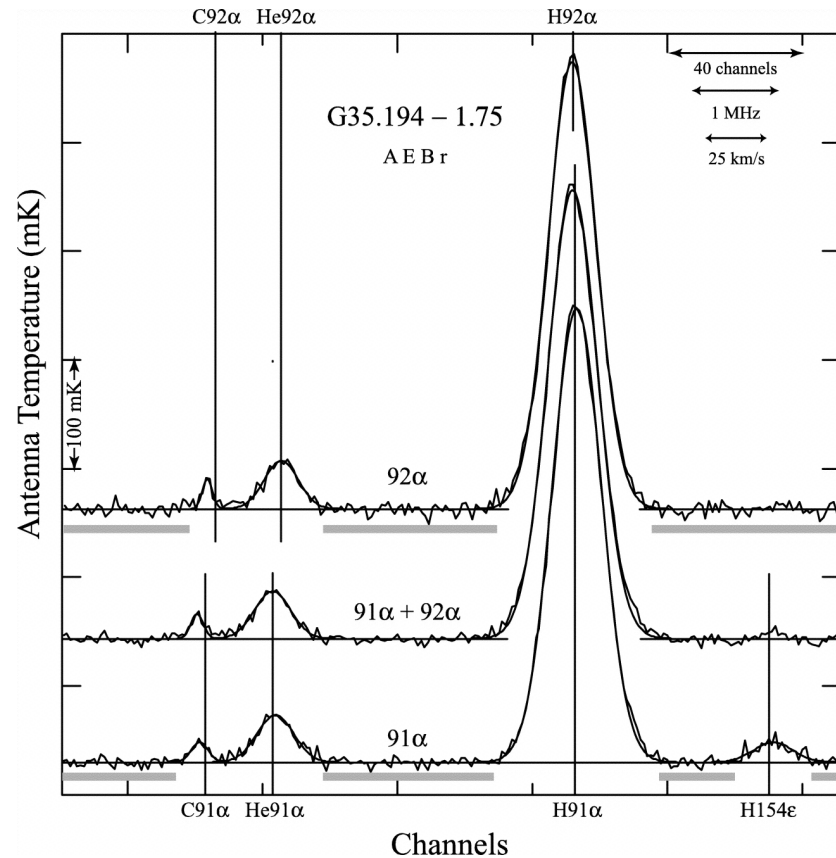
Advantages to using radio recombination lines for studying chemical evolution

- Mostly unaffected by interstellar extinction, so can (if the features are strong enough) probe the full range of galactocentric distance.
- Optically-thin line formation, so easier to extract abundances, especially relative abundances.



C. Esteban et al., 'Carbon and Oxygen Galactic Gradients: Observational Values from HII Region Recombination Lines,' *Astrophys. J Lett.*, **618**, L95-L98 (2005)

Direct comparison of abundances from $Hn\alpha$ and $Cn\alpha$ are thwarted by disjoint line formation regions



Quireza *et al.* 2006, *ApJS*, **165**, 338
[NRAO ASTR 534]

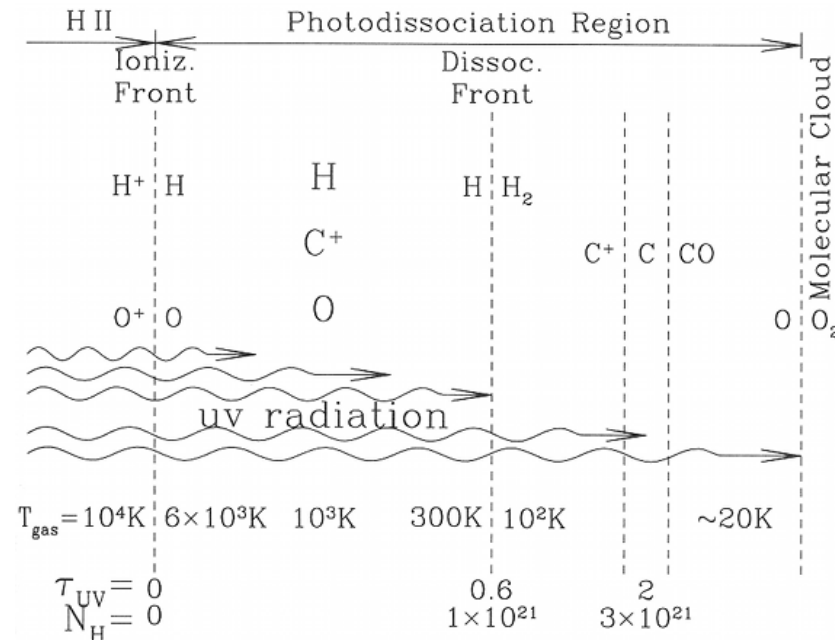


Figure 31.2 Structure of a PDR at the interface between an H II region and a dense molecular cloud.

Bruce T. Draine, *Physics of the interstellar and intergalactic medium*, (Princeton: Princeton University Press, 2011), p. 353.

Ionization potentials (eV)

Z	Element	Spectrum													
		I	II	III	IV	V	VI	VII	VIII	IX	X	XI			
1	H	13.598													
2	He	24.587	54.416												
3	Li	5.392	75.638	122.451											
4	Be	9.322	18.211	153.893	217.713										
5	B	8.298	25.154	37.930	259.368	340.217									
6	C	11.260	24.383	47.887	64.492	392.077	489.981								
7	N	14.534	29.601	47.448	77.472	97.888	552.057	667.029							
8	O	13.618	35.116	54.934	77.412	113.896	138.116	739.315	871.387						
9	F	17.422	34.970	62.707	87.138	114.240	157.161	185.182	953.886	1103.089					
10	Ne	21.564	40.962	63.45	97.11	126.21	157.93	207.27	239.09	1195.797	1362.164				
11	Na	5.139	47.286	71.64	98.91	138.39	172.15	208.47	264.18	299.87	1465.091	1648.659			

I.P.(He → He⁺) ≈ I.P.(C⁺ → C⁺⁺)

When the ionizing source is hot enough, the Strömgren spheres for higher ionization-potential ions overlap the Strömgren sphere for hydrogen.

Osterbrock, D. E., and Ferland, G. J., *Astrophysics of Gaseous Nebulae and Active Galactic Nuclei*, 2nd ed, (Sausalito CA: University Science Books, 2006).

$$\int_{IP}^{\infty} \frac{L_{\nu}}{h\nu} d\nu = \frac{4\pi}{3} R^3 n^2 \alpha_B$$

Total recombination coefficient into all but ground state

- If photons with $h\nu > 24.6$ eV are a small fraction of the total,
 - then the photons with 13.6 eV $> h\nu > 24.6$ eV will be used up in sustaining the ionization of hydrogen,
 - and those with $h\nu > 24.6$ eV will be used to ionize helium.
- If photons with $h\nu > 24.6$ eV are a large fraction of the total, then they will dominate both the ionization of hydrogen and the ionization of helium.

Fraction of $h\nu > 24.6$ eV vs spectral type

- What we want to target, then, are HII regions whose exciting stars are spectral class O6 or hotter.

Bruce T. Draine, *Physics of the interstellar and intergalactic medium*, (Princeton: Princeton University Press, 2011), p. 174.

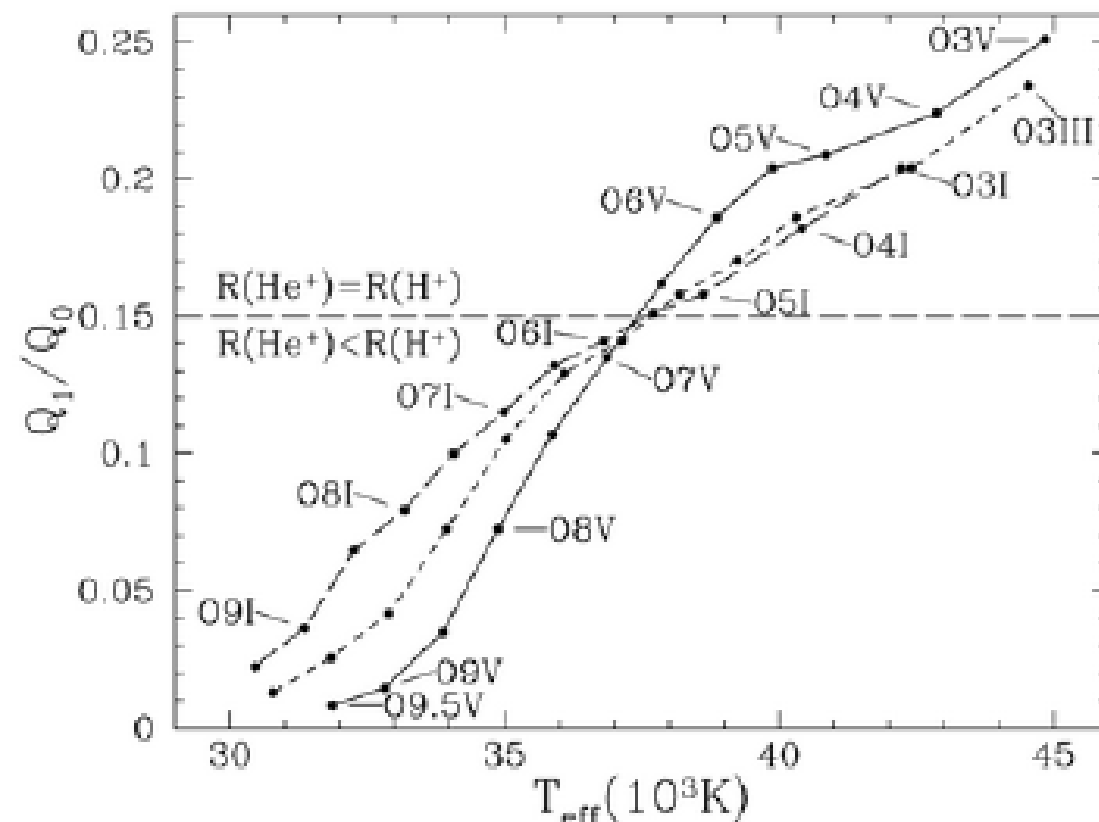
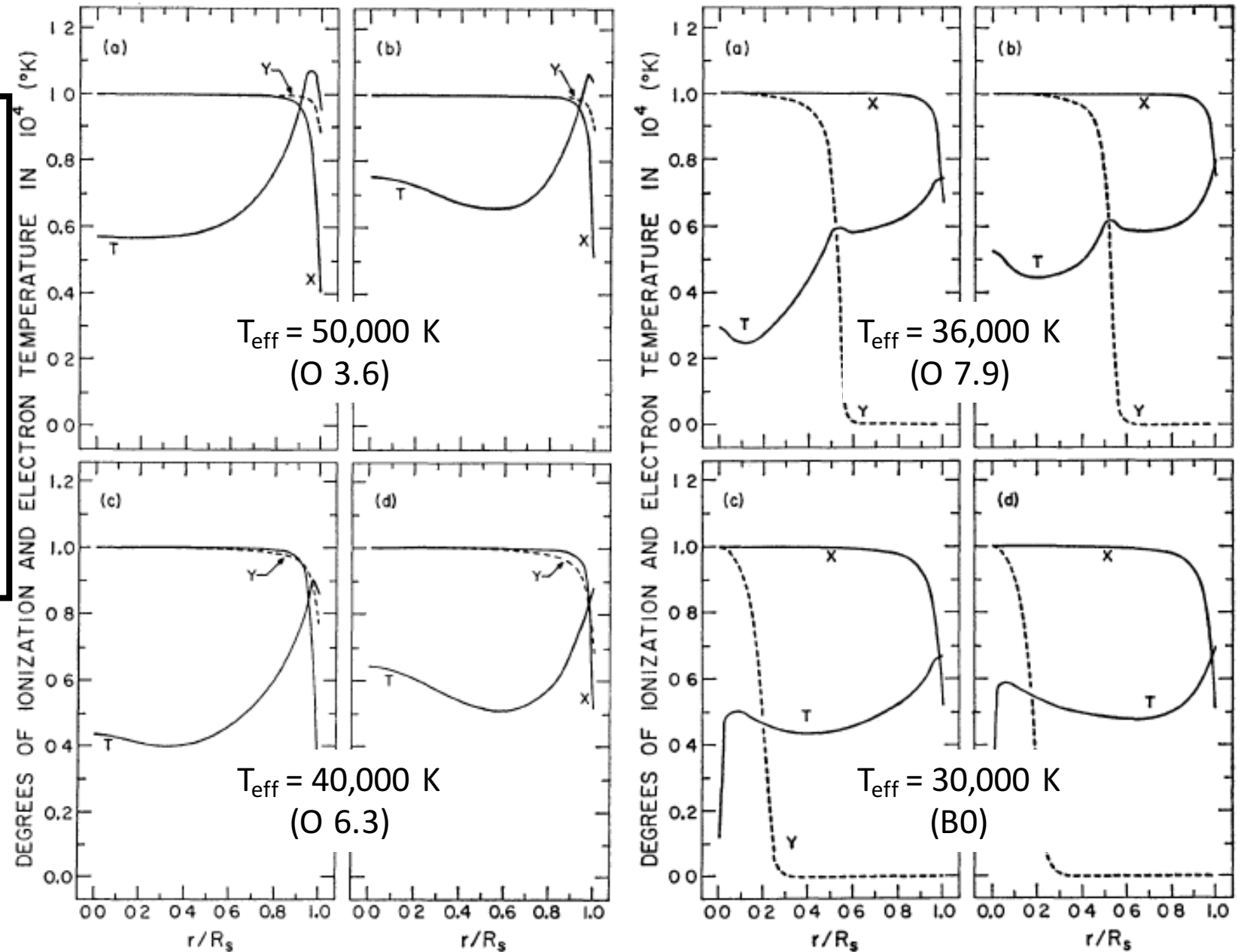


Figure 15.5 Q_1/Q_0 = ratio of rate of emission of $h\nu > 24.6$ eV photons to rate of emission of $h\nu > 13.6$ eV photons, as a function of T_{eff} , for luminosity classes V, III, and I (see Table 15.1). $Q_1/Q_0 \gtrsim 0.15$ is required for He to be ionized throughout the HII region, corresponding to $T_{\text{eff}} \gtrsim 37,000$ K.

When the ionizing source is hot enough, the Strömgren spheres for higher ionization-potential ions overlap the Strömgren sphere for hydrogen.

R. H. Rubin, 'The Structure and Properties of HII Regions,' *Astrophys. J.*, **153**, 761-782 (1968)



If C⁺⁺ and He⁺ are essentially coexistent...

- Could search for C⁺nα recombination lines, found at 4 times the frequency of the Cnα recombination lines:

$$\nu_n = cZ^2R \left(1 - \frac{m_e}{M_C}\right) \left[\frac{1}{n^2} - \frac{1}{(n+\Delta n)^2}\right]$$

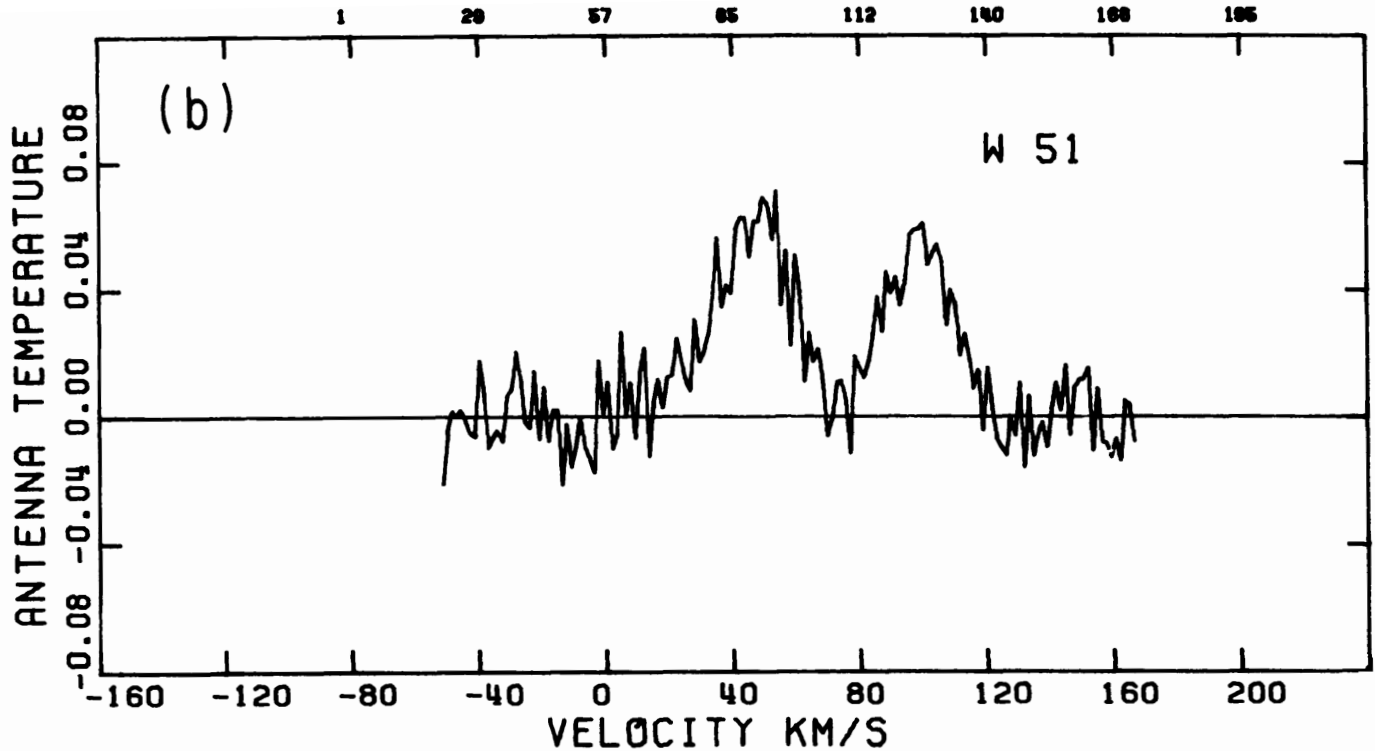
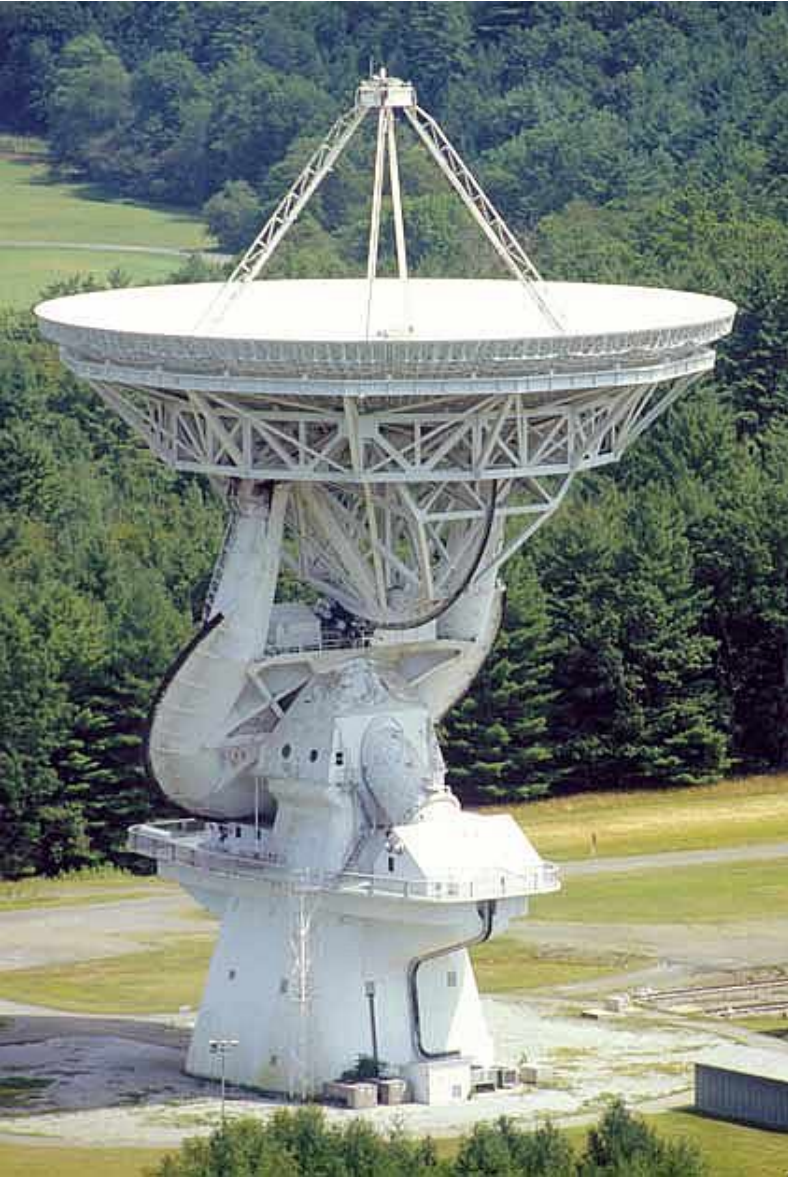
- If scale to apparent optical depth of He emission:

$$\frac{(T_L/T_C)_{C^+}}{(T_L/T_C)_{He}} = \frac{[C]}{[He]} \frac{b(C^+)}{b(He)} \frac{\{1 - \tau_C \beta(C^+)/2\}}{\{1 - \tau_C \beta(He)/2\}}$$

Departure coefficient, defined as the deviation of the energy level populations from LTE

Slope of the variation, with n, in departure coefficients

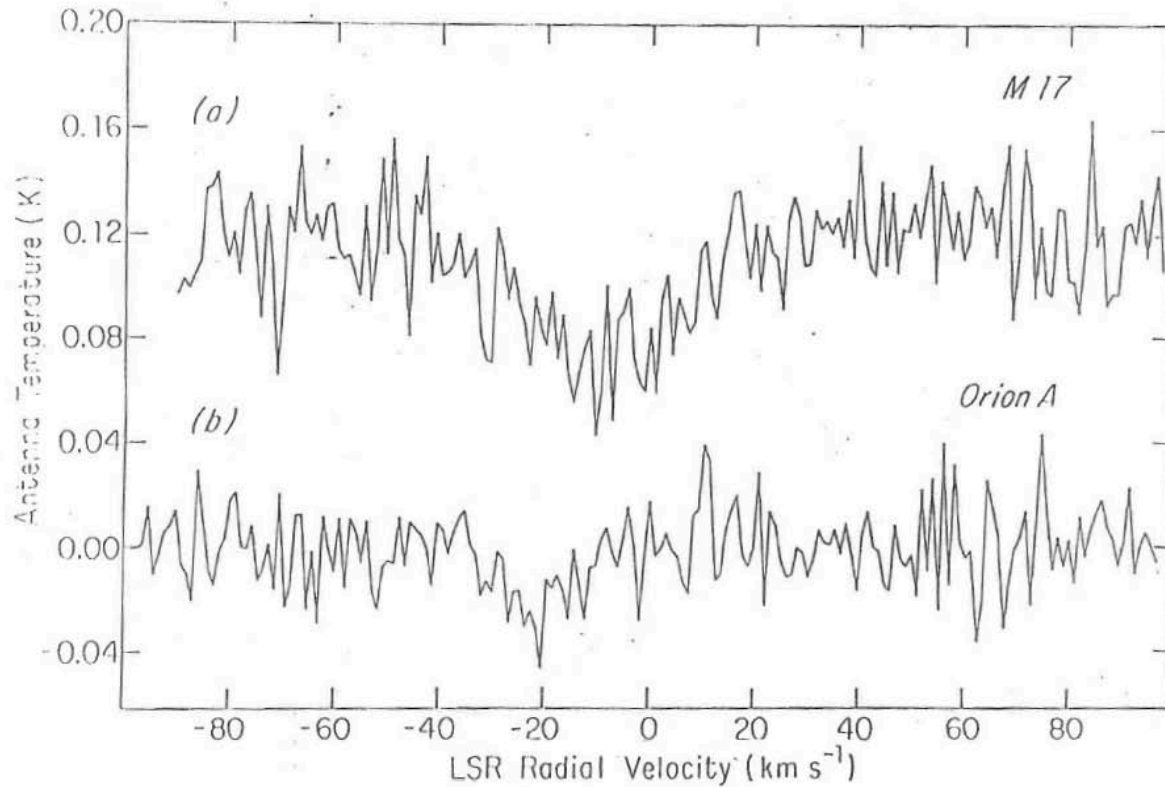
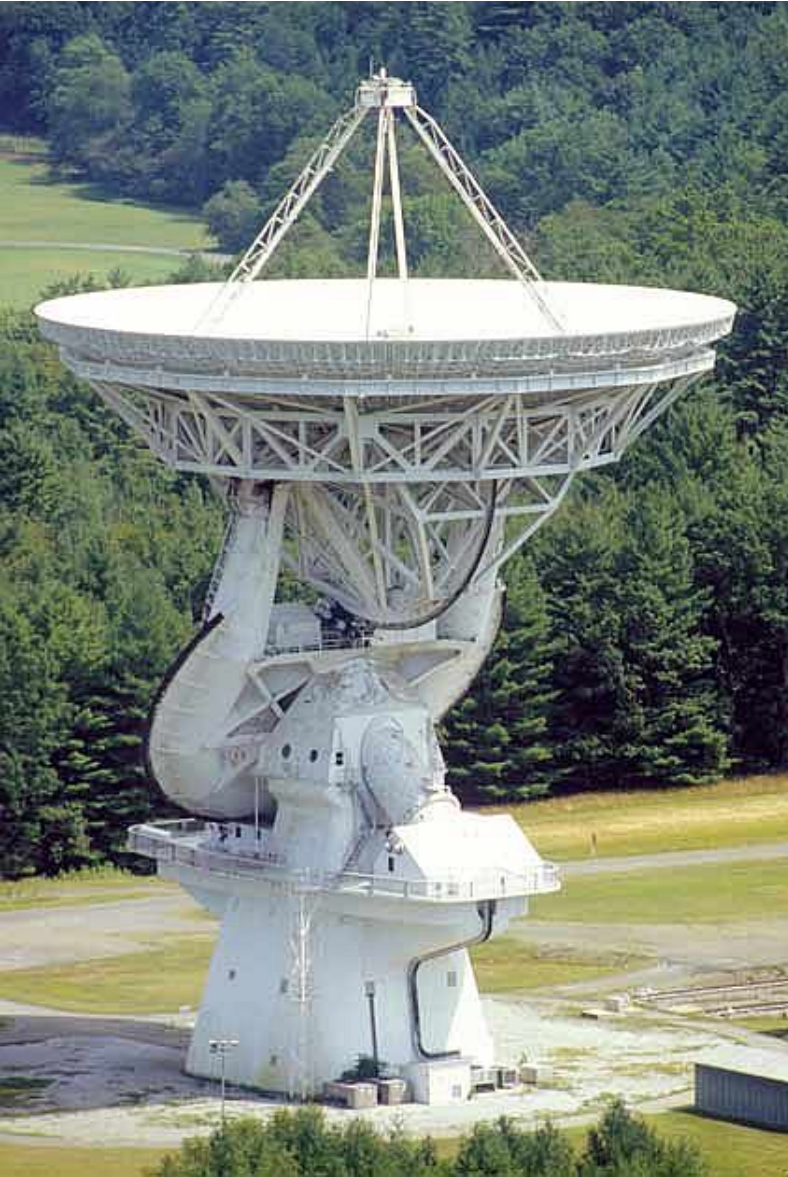
Original Searches at Green Bank 140' Telescope



"C⁺134 α " and "He⁺134 α " at 10.82 GHz, 29 August 1976

F. J. Lockman and L. J. Rickard, *NRAO Green Bank Electronics Division Internal Report No. 183*, 'Spurious Spectral Features at the 140-foot Telescope' (12/77)

Original Detections at Green Bank 140' Telescope



Spectral Class
of exciting stars

O4 – O5

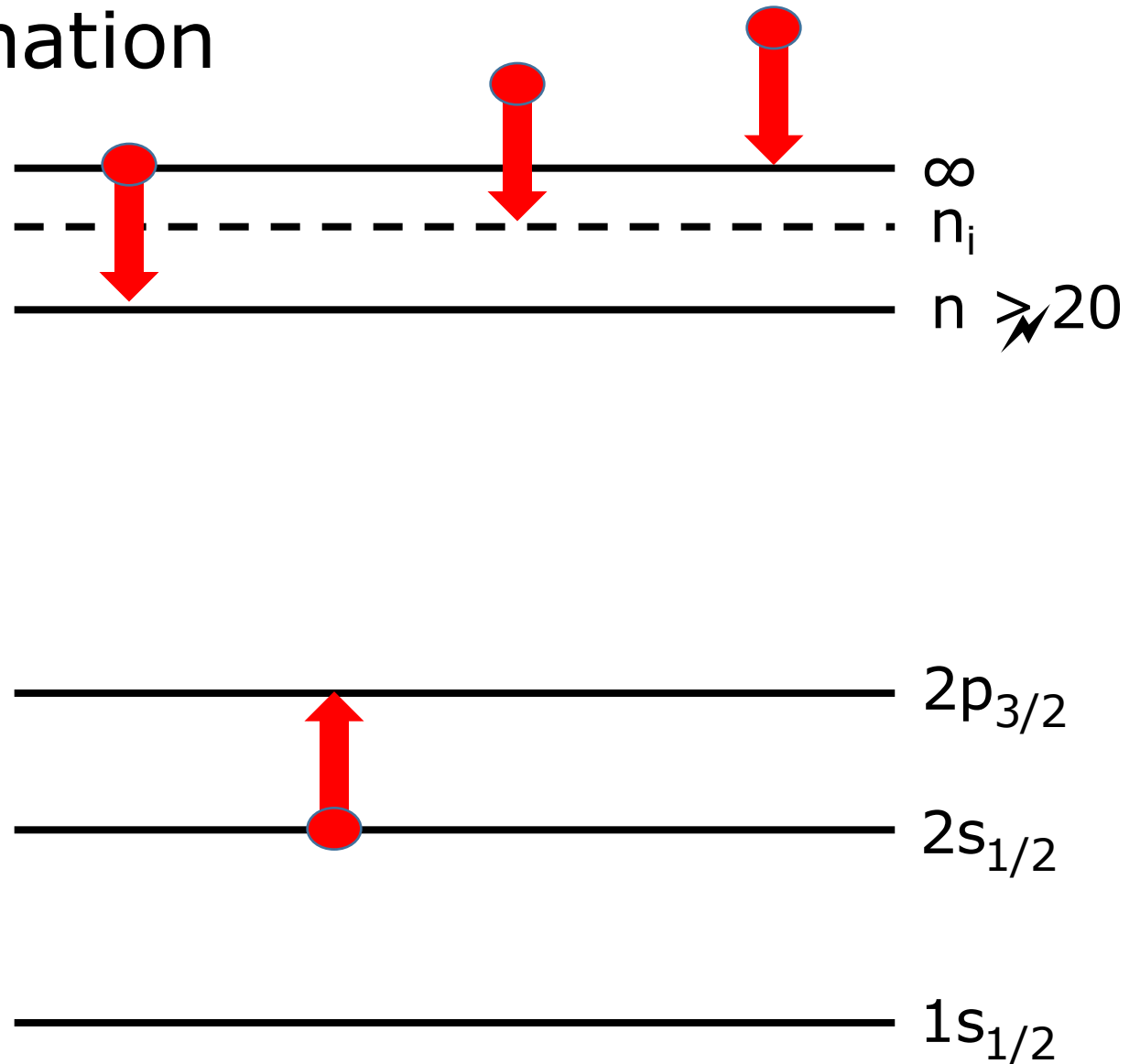
O6

C⁺265 α features at 1.4 GHz

Rickard, L. J, *Bull. Amer. Astr. Soc.*, **14**, 913 (1982)

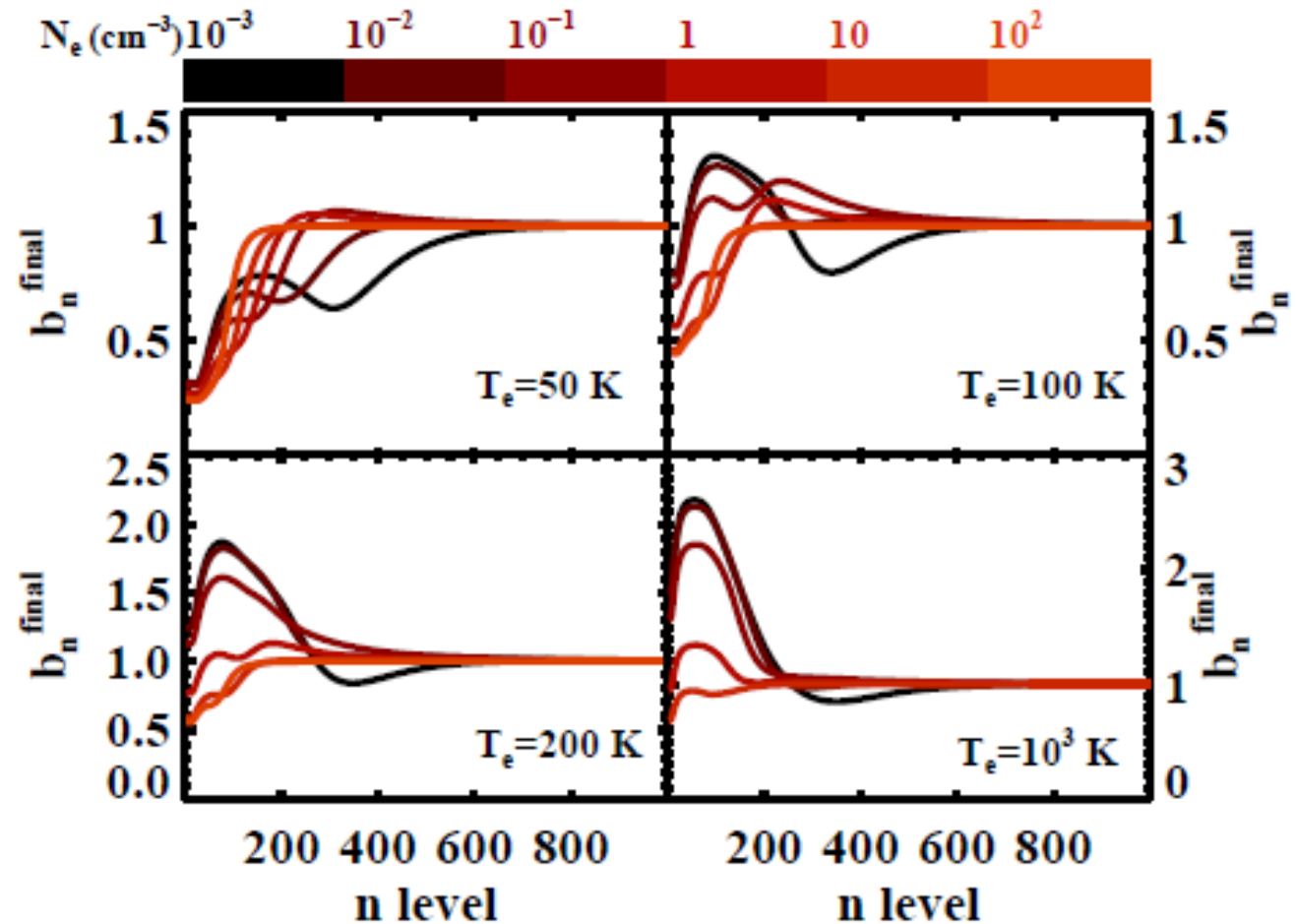
Why absorption? Dielectronic recombination

- Because the lowest electronic states are complex, and,
- Particularly, because of the presence of fine-structure splitting,
- Can balance the energy to be given up in recombination by that needed to excite the fine-structure transition.



Dielectronic recombination

- Convolution of the energy constraint with the Maxwellian distribution in the continuum can produce huge bulges in departure coefficients.



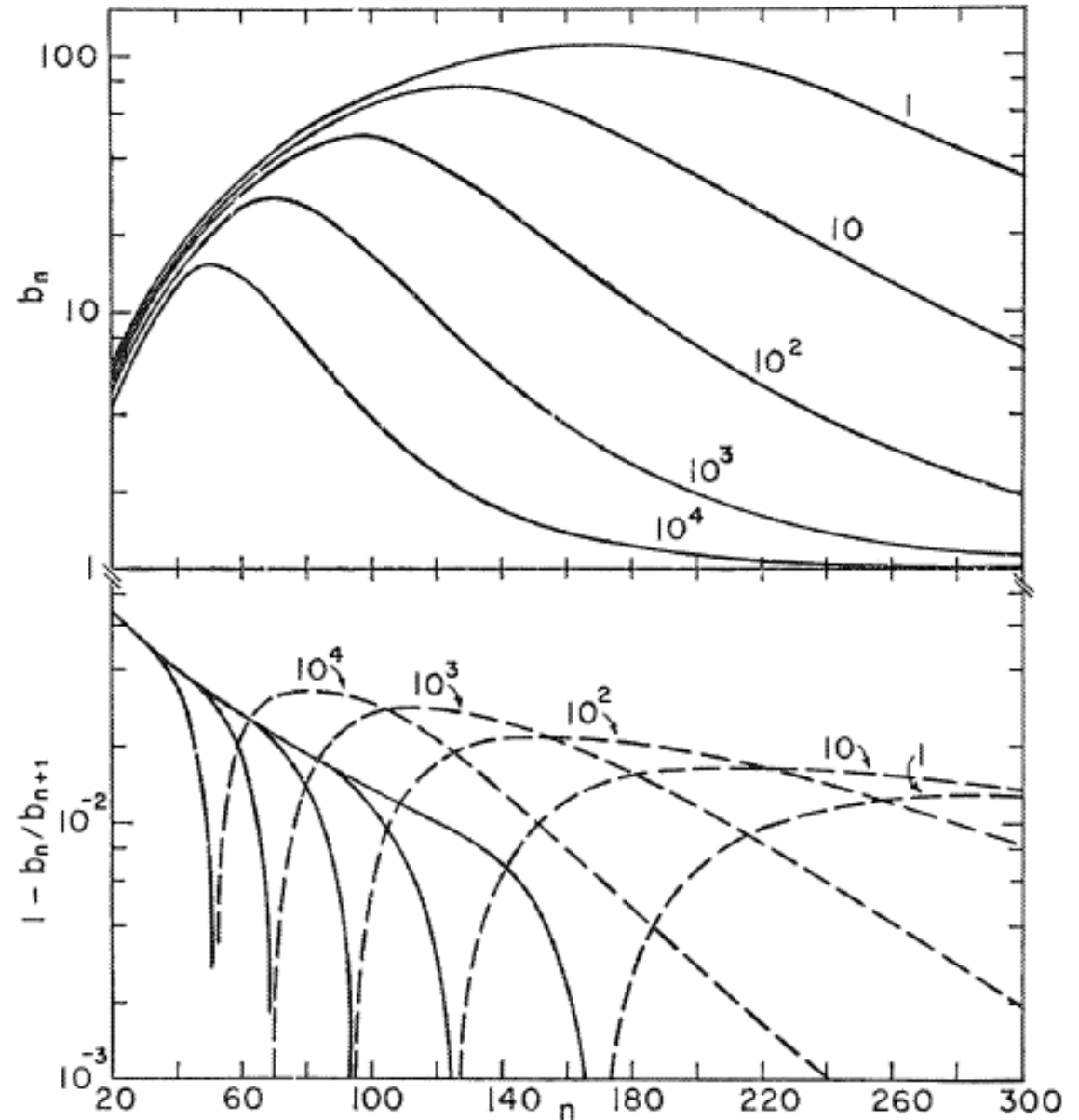
F. Salgado et al., 'Low Frequency Carbon Radio Recombination Lines I: Calculations of Departure Coefficients,' arXiv 1609.06938v1

Fig. 6.— Final departure coefficients for carbon atoms (b_n^{final}) as a function of n level at $T_e = 50, 100, 200$ and 1000 K for different densities (N_e , colorscale). The “bump” seen in hydrogenic atoms is amplified by dielectronic recombination. As density increases the b_n^{final} are closer to the hydrogenic value.

Dielectronic recombination

- $n(\text{peak } b_n)$ is lower for higher n_e .
- $n(\text{peak } b_n)$ marks transition point between enhanced stimulated emission and enhanced absorption.

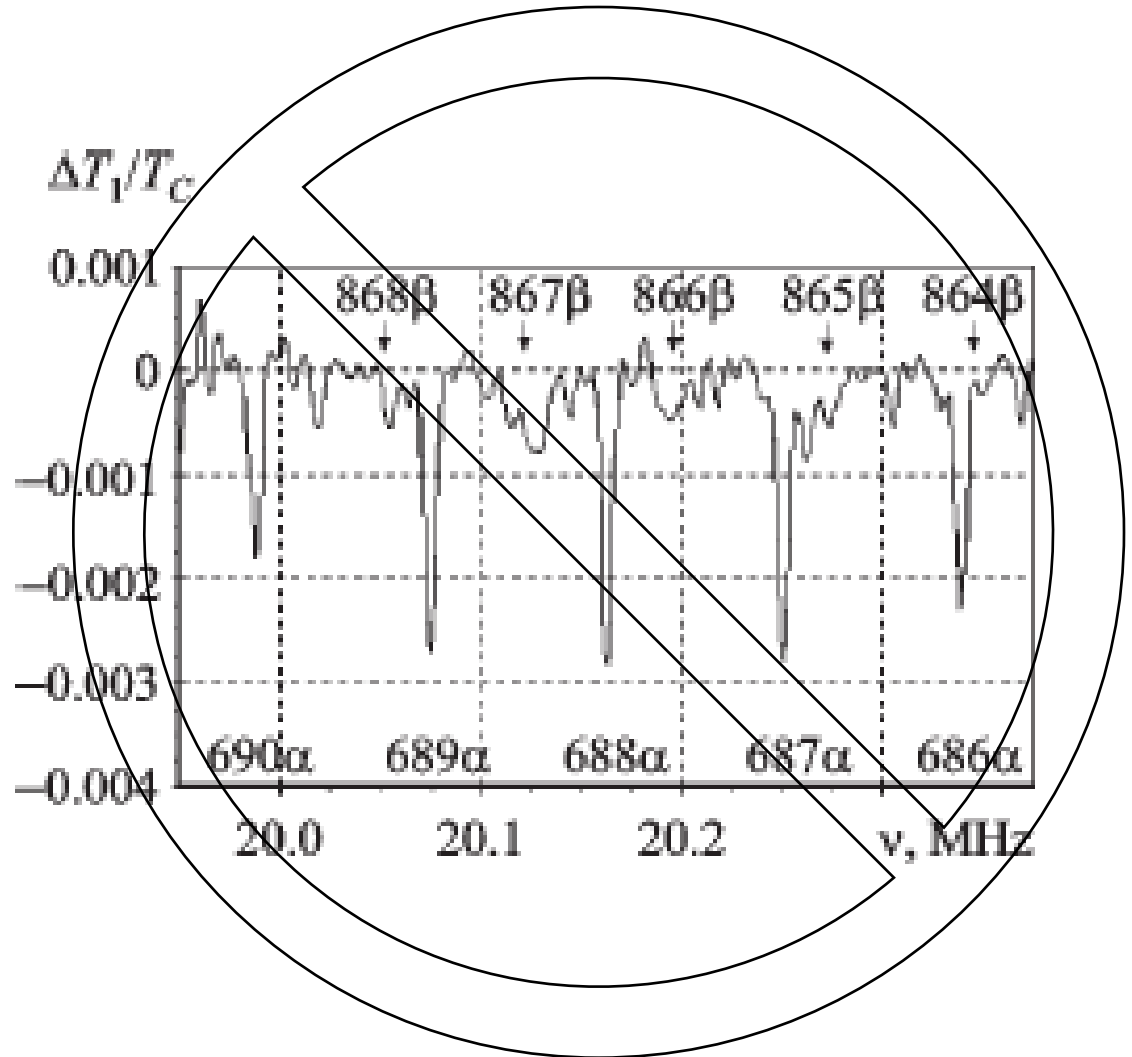
A. K. Dupree, 'Radio Recombination Lines from Heavy Elements: Carbon,' *Astrophys. J.*, **158**, 491-503 (1969)



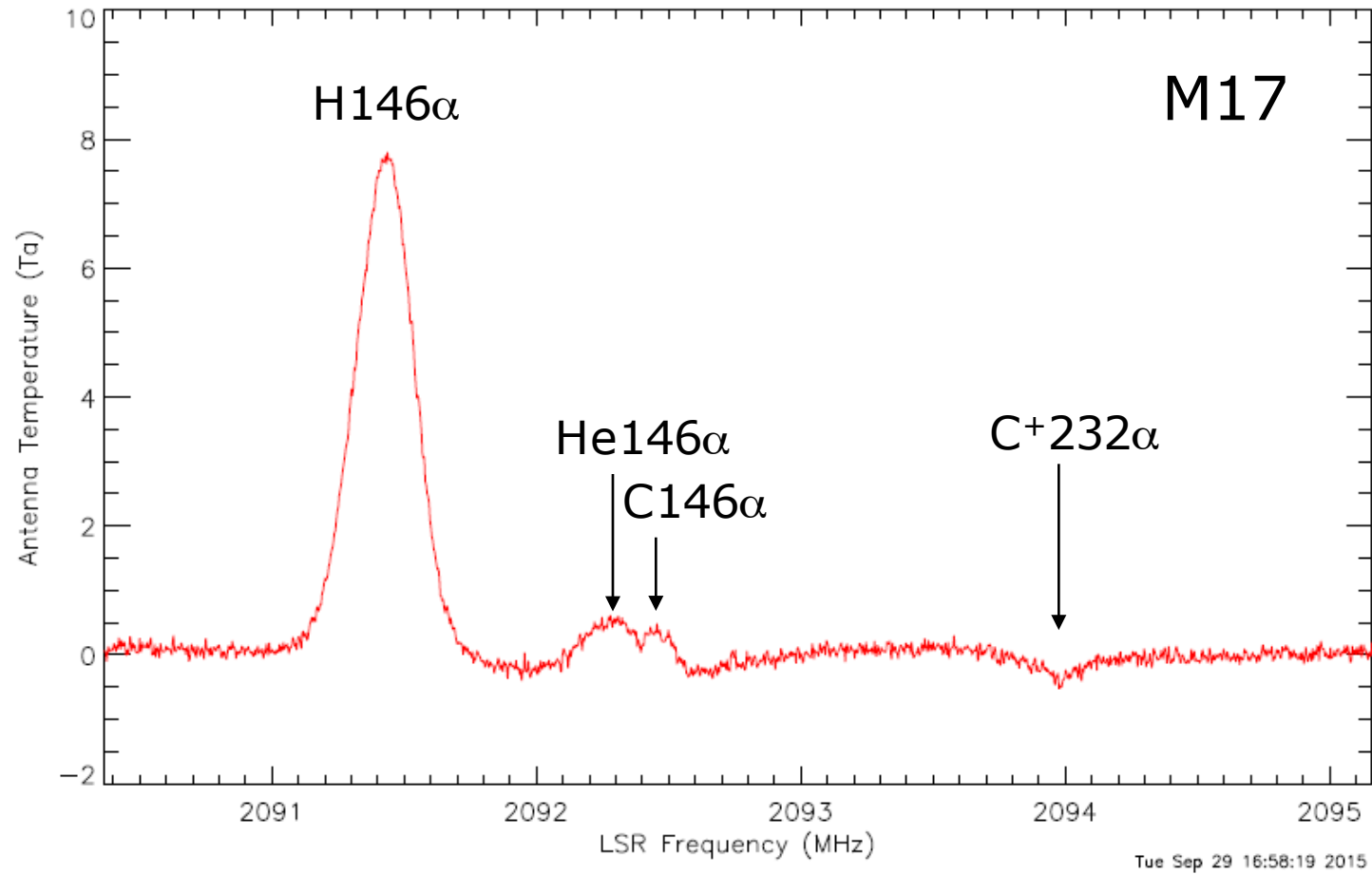
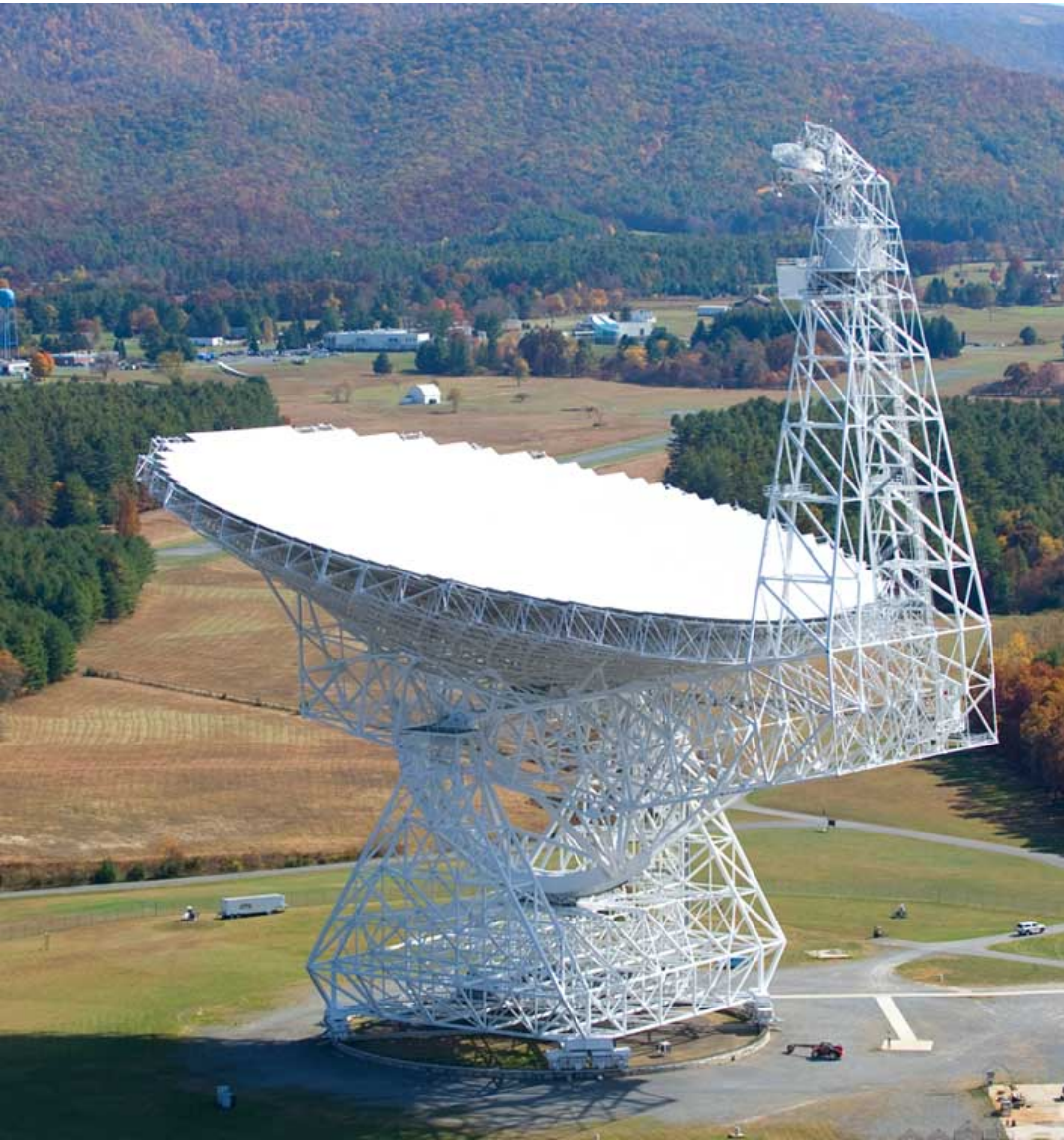
This is different than the $Cn\alpha$ absorption seen at low frequencies.

- Dielectronic recombination is dominant in both cases.
- Low frequency $Cn\alpha$ are diffuse ISM features, not HII region features.
- Temperatures are low, densities are very low, n-values are very high.

A. A. Konovalenko, S. V. Stepkin, and D. V. Shalunov,
'Low-Frequency Carbon Recombination Lines,'
Radiophys. Radioastron., **6#1**, 1-11 (2001).



Recent Detections at Green Bank Observatory



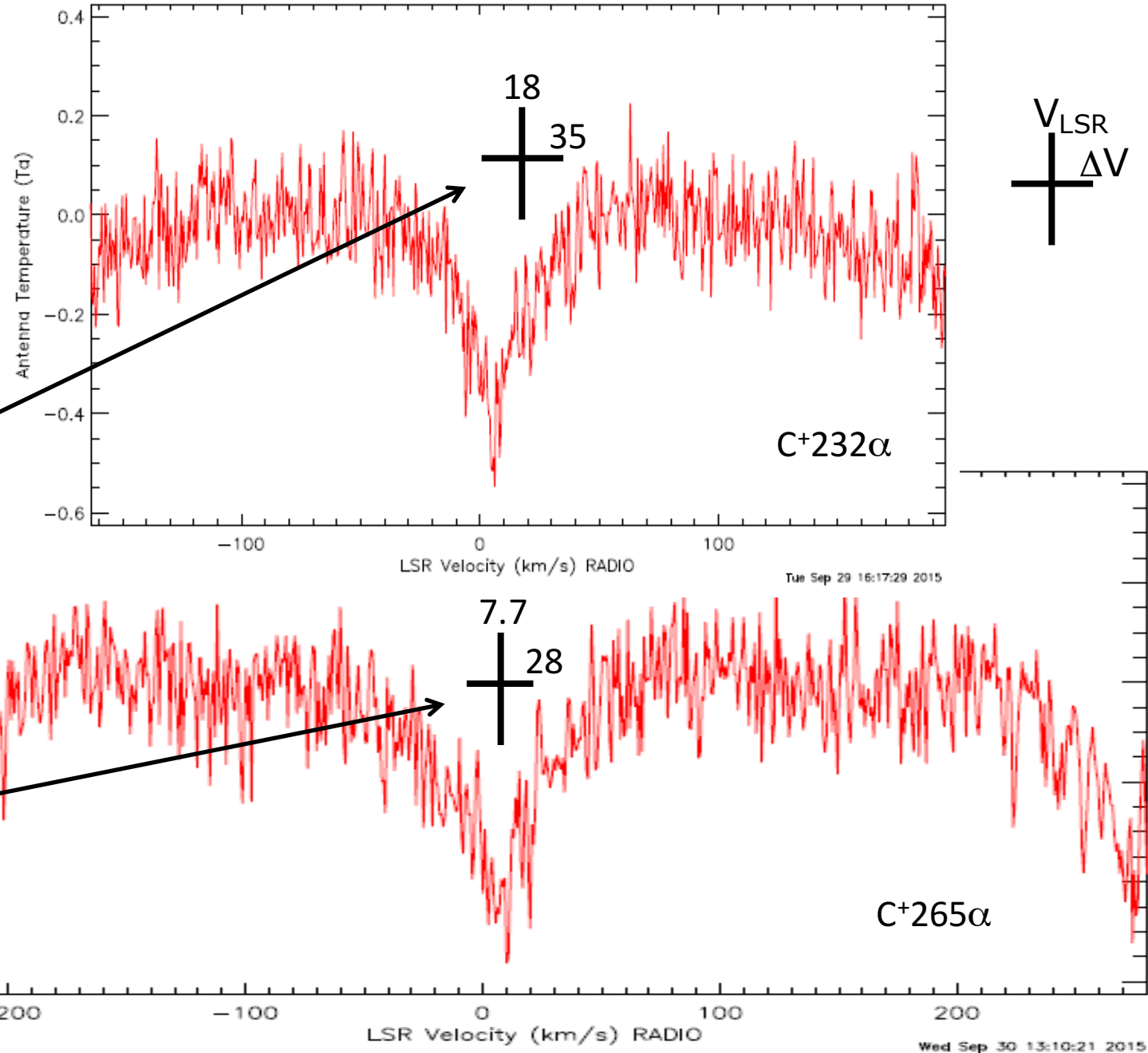
With Bridget McEwen and Ylva Pihlstrom

All data... so far

Source		n	$-T_L$		T_C		V_{LSR}		Δv		RMS	Apparent Optical Depth	
			(K)	error	(K)	error	(km/s)	error	(km/s)	error	(K)	$-1000 \times T_L/T_C$	error
M 17		295	0.059	0.007	162	9	8.5	2.3	40	6	0.0264	0.364	0.048
	140	282	0.32 ^a	0.054	617 ^b	19	8.4	2.2	24	6	0.1147	0.519	0.089
	GBT	271	0.561	0.039	617 ^b	19	10.0	1.1	33	3	0.1407	0.909	0.069
	140	266	0.060	0.005	159	2	10.0	1.3	35	3	0.0208	0.377	0.032
	140	265	0.054	0.007	153	2	7.7	1.7	28	4	0.0213	0.353	0.046
	GBT	265	0.359	0.017	617 ^b	19	4.0	1.0	52	2	0.0795	0.582	0.033
	140	247	0.080	0.010	154	2	11.8	1.8	30	4	0.0148	0.519	0.065
	GBT	245	0.294	0.016	443 ^b	13	8.0	0.9	33	2	0.0841	0.664	0.041
	GBT	232	0.357	0.013	443 ^b	13	6.6	0.6	35	1	0.0676	0.806	0.038
	140	224	0.051	0.009	126	4	10.7	1.8	20	4	0.0284	0.405	0.073
140	200	0.030	0.002	116	2	7.2	1.5	36	3	0.0106	0.259	0.018	
Orion A	140	295	0.014	0.003	99	6	-19.1	5.2	45	15	0.0125	0.141	0.031
	140	266	0.011	0.003	106	1	-20.0	4.3	29	11	0.0130	0.104	0.028
	140	265	0.032	0.005	102	2	-21.2	1.0	14	3	0.0179	0.314	0.049
	140	247	.02? ^a		105	8	(-12)		(10)		0.0160	0.2?	
	140	224	.02? ^c		96	4	(-16)		(9)		0.0221	0.2?	
	140	200	0.014	0.002	96	3	-11.3	2.4	33	6	0.0087	0.146	0.021
			^a Transition obscured by interference										
			^b Measured over same broad band										
			^c Marginal detection										

Feature parameters

- $\langle V_{\text{LSR}} \rangle = (7.6 \pm 0.3) \text{ km/s}$
- $\langle \Delta V \rangle = (36 \pm 1) \text{ km/s}$
- Blue-shifted from He
 - e.g., $V(\text{He}86\alpha) = 18 \text{ km/s}$
- Where in common, GBT and 140' data are in agreement.

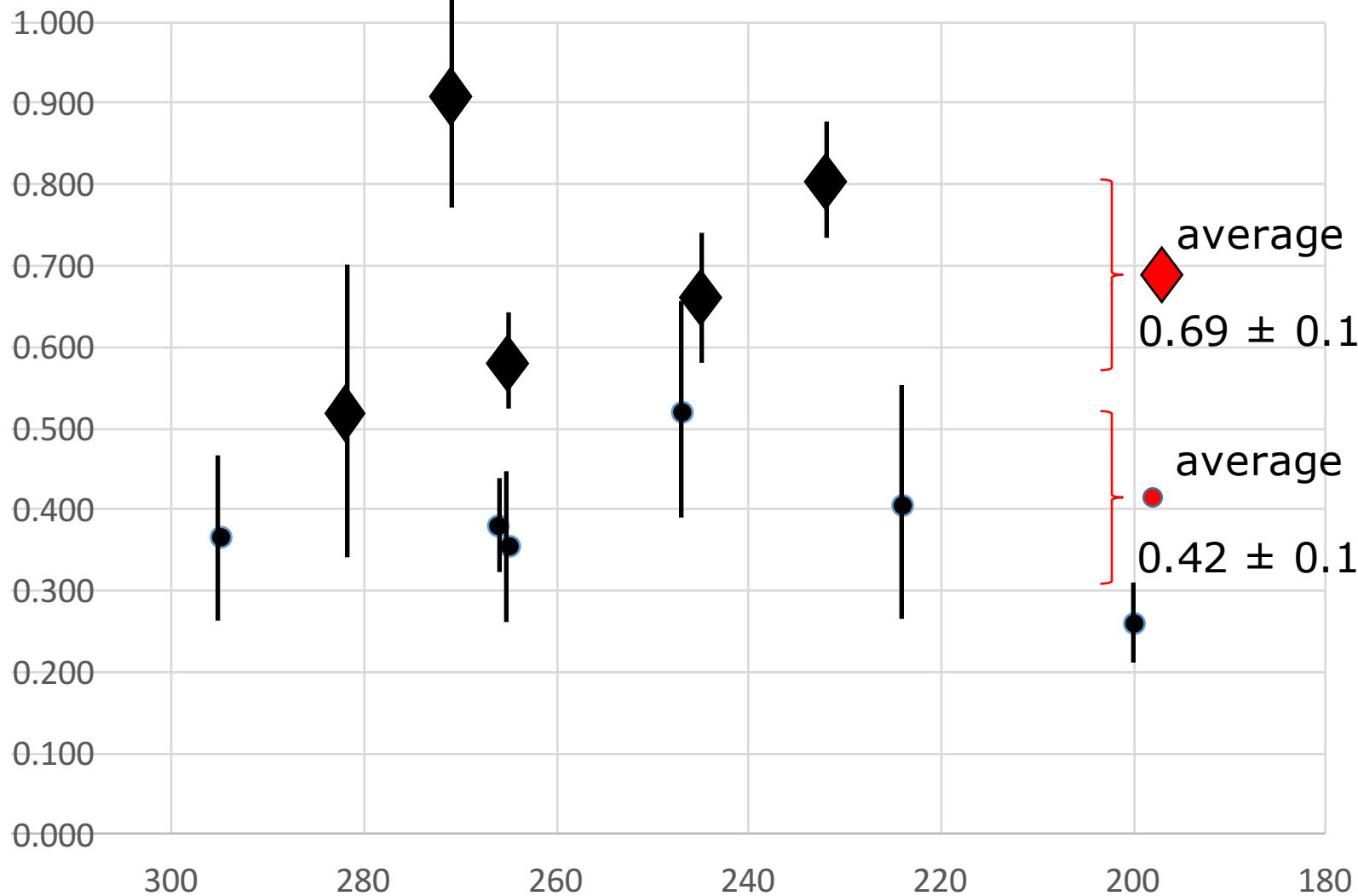


Offsets from emission features

- Collected a set of 13 measurements of $Hn\alpha$ towards M17S
 - Added three GBT measurements: $n = 146, 167, \text{ and } 178$
 - Weighted average: $\langle V(H) \rangle = (13.8 \pm 4.8) \text{ km/s}$
- Collected a set of 7 measurements of $He n\alpha$ towards M17S
 - Two lacked error estimates
 - Added GBT measurement for $n = 146$
 - Weighted average: $\langle V(He) \rangle = (12.4 \pm 5.0) \text{ km/s}$
- Compare with $\langle V(C^+) \rangle = (7.6 \pm 0.3) \text{ km/s}$
- Similarly, $\langle \Delta V(H) \rangle = (41.0 \pm 6.7) \text{ km/s}$, $\langle \Delta V(He) \rangle = (22.6 \pm 4.5) \text{ km/s}$
- Compare with $\langle \Delta V(C^+) \rangle = (22.6 \pm 4.5) \text{ km/s}$

M17 - C⁺na - Apparent Optical Depths

Apparent Optical Depth ($- \tau_L / \tau_c$) (x 1000)



◆ - GBT

● - 140

error bars
are $\pm 2\sigma$

average

0.69 ± 0.12

average

0.42 ± 0.11

What needs to be done next

- Search for features at $n \leq 200$ ($\nu \geq 3.3$ GHz), to find the turnover from absorption to emission.
- Search additional sources, starting with Orion A.
- Do detailed calculations to see what the implied [C]/[He] results are.
 - Current GBT results are within order of magnitude of standard [C]/[He].
- Refine measurements of apparent optical depth using EVLA.

Backup

Radio Recombination (High Rydberg State) Lines

Energy-level diagram for hydrogen

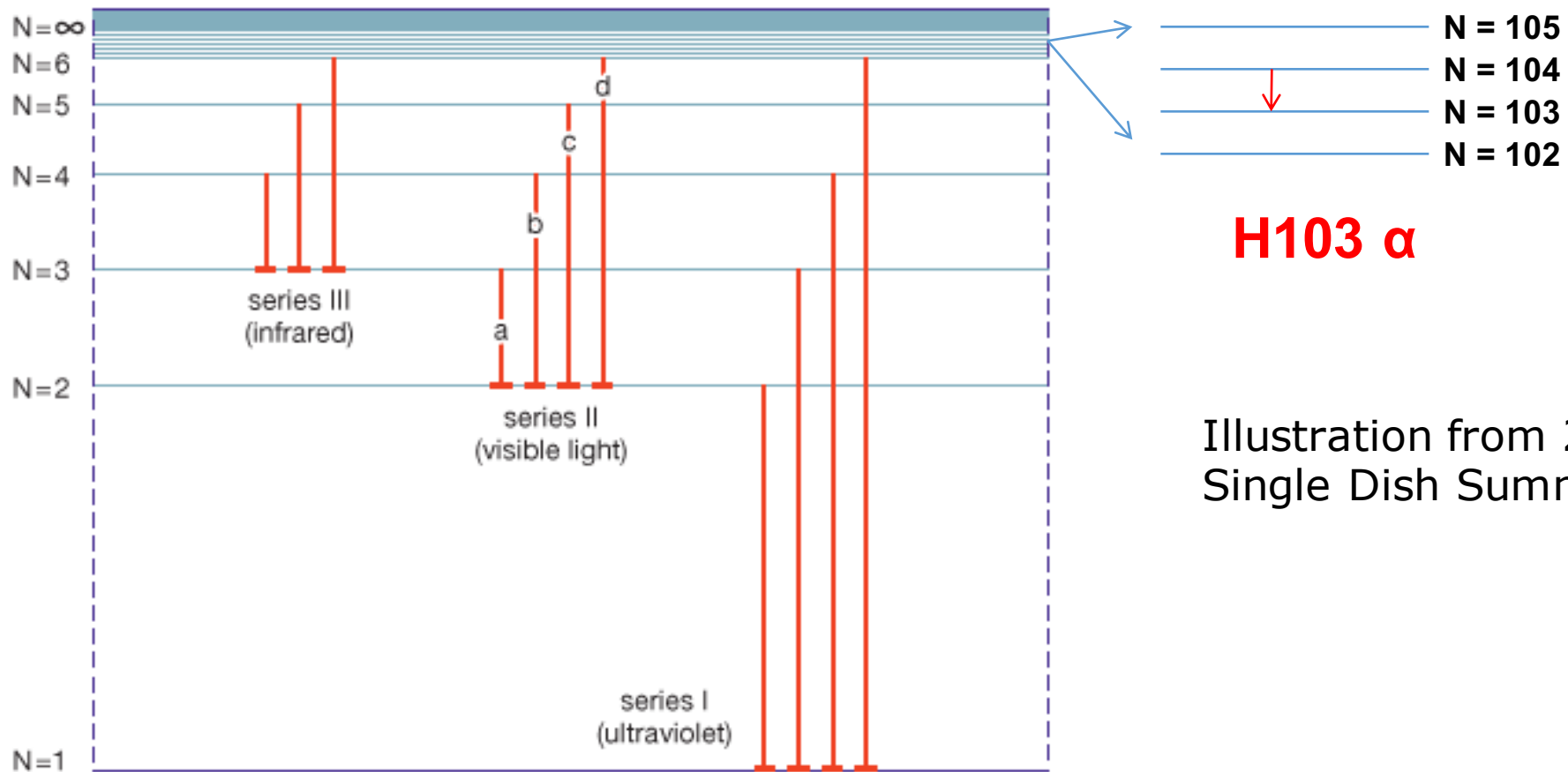


Illustration from 2009 NRAO
Single Dish Summer School

Purely radiative recombination

- Can have structure in departure coefficients, leading to
- Significant negative values of departure slope (β), leading to
- Significant contribution of stimulated emission to total emission.

F. Salgado et al., 'Low Frequency Carbon Radio Recombination Lines I: Calculations of Departure Coefficients,' arXiv 1609.06938v1

Note that the b_n go to unity (LTE) when collisions dominate.

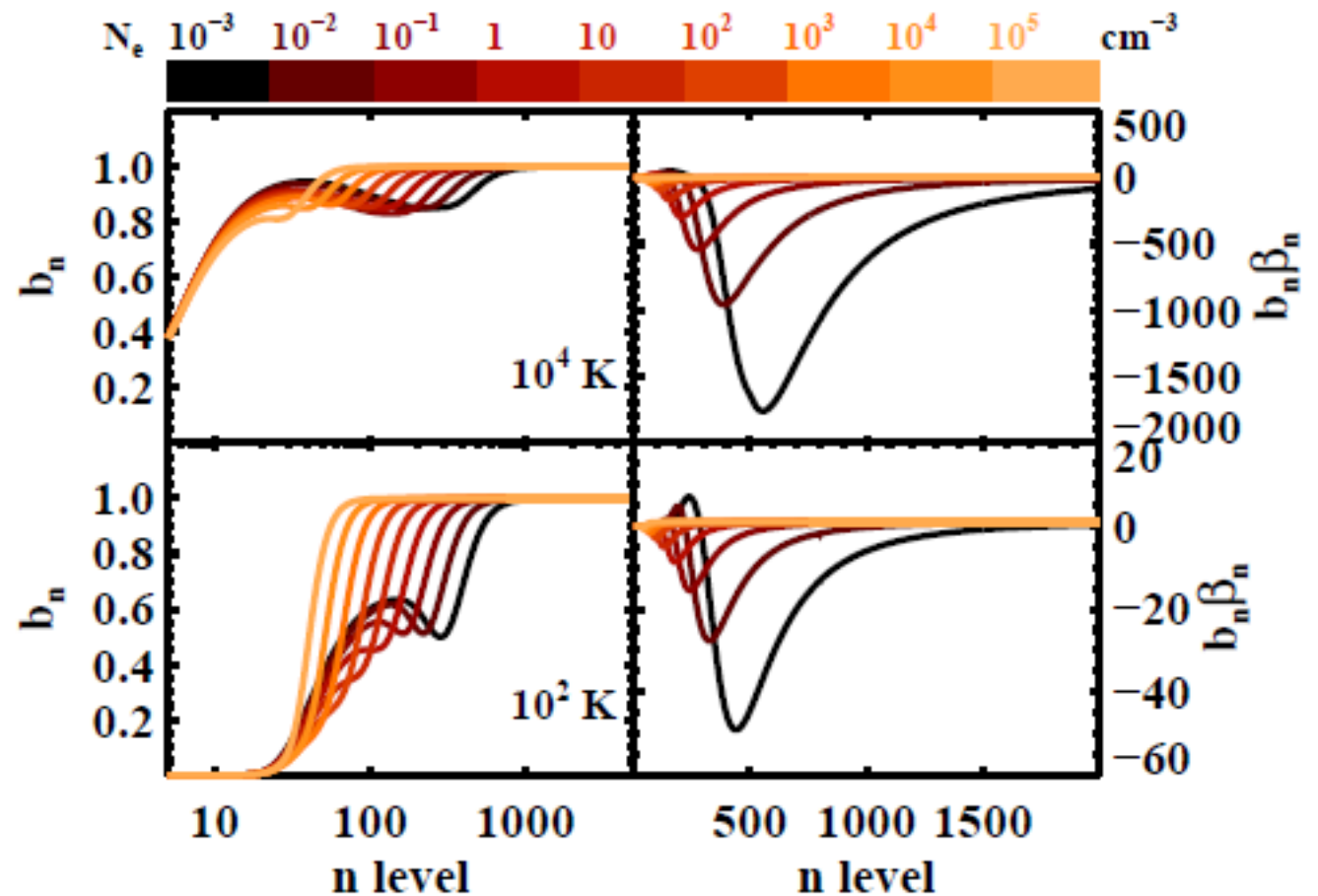


Fig. 3.— b_n values (left) and $b_n \beta_n$ values (right) for hydrogen at $T_e = 10^4$ and 10^2 K (upper and lower panels, respectively) for different densities (N_e , colorscale). The departure coefficients obtained using the nl -method show a “bump” at low n levels. The strength and position of the “bump” depend on the physical conditions. As density increases, the l -changing collisions redistribute the electron population more effectively.

Dielectronic recombination

- Can get large negative and positive $b_n\beta_n$
- Note that, for sufficiently high temperatures and densities, there is no crossover from positive $b_n\beta_n$ to negative $b_n\beta_n$.

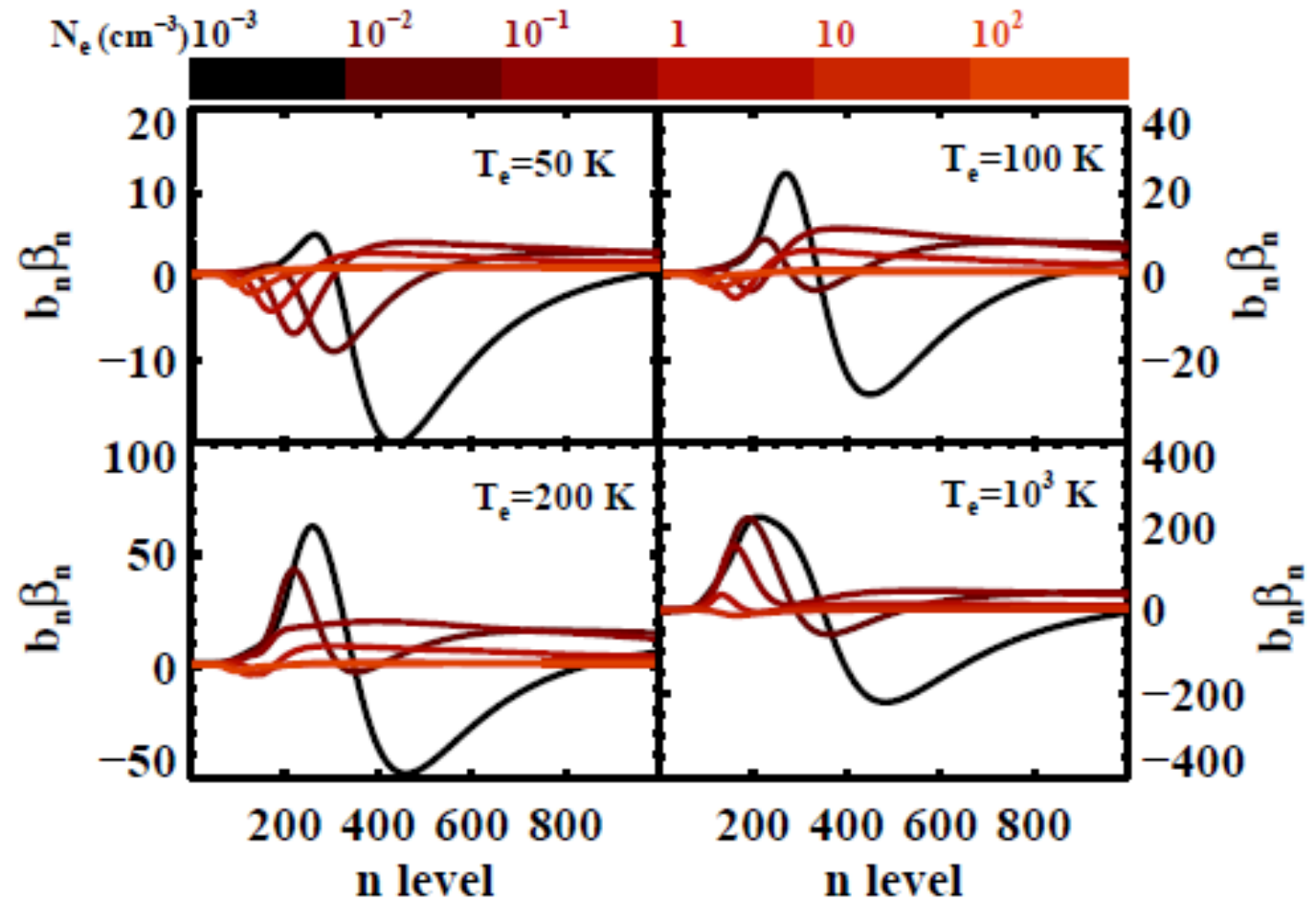


Fig. 8.— $b_n\beta_n$ values for carbon atoms at $T_e = 50, 100, 200$ and 1000 K for different densities (N_e , colorscale).

F. Salgado et al., 'Low Frequency Carbon Radio Recombination Lines I: Calculations of Departure Coefficients,' arXiv 1609.06938v1